Available online at http://scik.org

J. Math. Comput. Sci. 10 (2020), No. 6, 2634-2657

https://doi.org/10.28919/jmcs/4961

ISSN: 1927-5307

MAGNETOHYDRODYNAMIC WILLIAMSON FLUID MOTION OVER AN EXPONENTIALLY STRETCHING SHEET WITH CHEMICALLY RADIATIVE HEAT SOURCE EFFECTS UNDER SUCTION/INJECTION

ABBURI SREENIVASA RAO[1,*], PEDDI PHANI BUSHAN RAO[2], CHARAN KUMAR GANTEDA[3]

[1]Department of Mathematics, Coastal Institute of Technology and Management, Kothavalasa, AP, India

[2]Department of Mathematics, Institute of Science, Gitam Deemed to be University, Visakhapatnam, AP, India

[3]Department of Mathematics, Koneru Lakshmaiah Education Foundation, Guntur, AP, 522510, India

Abstract: In this paper, the attitude priority of this expose is to investigate the scenery of the motion, thermal and mass transport of chemically reacting magnetohydrodynamic Williamson fluid with thermal radiation and heat source over an exponentially stretching surface through suction/injection. Leading equations are evolved and converted to ordinary differential equations using similarity techniques and solved by means of homotopy analysis method (HAM). The character of physical governing parameters on motion of liquid, temperature and concentration are discussed through numerical statistics and plots. Also the friction factor, local heat transport rate and local mass transport rate are premeditated to study the motion behavior at the wall. An association with penetrable grades for exacting cases is establish with remarkable assent.

Keywords: MHD; radiation; chemical reaction parameter; heat source; energy and stretching sheet.

2010 AMS Subject Classification: 76N16, 76N20.

*Corresponding author

E-mail address: asr161969@gmail.com

Received August 20, 2020

1. INTRODUCTION

Introduction. Non-Newtonian liquids are crucial in border stratum motions as of their manufacturing and expertise associated applications. Apple sauce, paints, ketchup, polymeric liquids, jellies, tomato sauce, glues, soaps, cosmetic commodities are examples of non-Newtonian liquids. As there are heterogeneity of non-Newtonian liquids so it is sensibly intricate to appearance an equation expressing the viscous and elastic properties of these liquids. In association to viscous liquids, mathematical modelling of non-Newtonian liquids is noticeably multifarious and challenging. Williamson fluid is feature of a non-Newtonian fluid replica with shear thinning belongings. This replica was planned by Williamson [1]. Nadeem and Hussian [2] discussed the Williamson fluid motion over an exponentially stretching sheet. Further details have been deliberated in [3-7].

Motion over stretching surfaces has gained plentiful significance in the investigation of border stratum motion due to its tremendous significance in manufacturing and developed sectors, such as wire drawing, hot rolling, paper manufacture, industrialized of rubber sheets, and glass blowing. Many years before, Serpa et al. [8] conducted an experimental investigation to scrutinize the disorderly alienated and reattached motion of a fluid. The isothermal slip motion due to stretching of a curved sheet was discussed by Barber et al. [9]. Shi and Liao [10] analyzed the motion and heat transport aspects of non-Newtonian fluids over a stretching surface. On the other hand, similar type of study on Newtonian fluids was reported by Sajid et al. [11]. Some authors (Naveed et al. [12], Hayat et al. [13], Saleh et al. [14], and Okechi et al. [15] scrutinized the heat transport individuality of fluid motion along a curved surface. All these authors utilized the well-known shooting procedure to attain the problem's solutions. Many studies accomplished that the fluid velocity is proportional to the curvature constraint.

Recently, considerable notice has been emphasized on exploitation of magnetohydrodynamics (MHD) and heat transport such as metallurgical processing, melt refining necessitates magnetic field applications to regulate exorbitant heat transport rate. Other applications of MHD heat transport include MHD generators, plasma thrust in astronautics, nuclear reactor thermal dynamics, ionized geothermal energy systems, etc. Abel et al. [16] discussed the motion and heat transport performance of viscoelastic fluid underneath the influence of viscous and ohmic dissipation over a stretching surface. Kumaran et al. [17] obtained the exact

solution for a border stratum motion of an electrically conducting fluid past a quadratically stretching and linearly permeable sheet. Fazle Mabood et al. [18] explained the thermal emission result on MHD motion above an exponentially stretching sheet. Siva Reddy et al. [19] have deliberated heat and mass transport effects on MHD natural convection motion past an impulsively moving vertical plate with ramped temperature. Later on many problems have been discussed by few authors [20-24].

The knowledge about heat transport has ample applications in the fields of engineering and paramedical. It also has environmental and industrial implications in the processes like power creation, heat exchangers, thermal conduction in tissues, electronic devices, and so on. Heat radiation is a process by which internal energy is transported through electromagnetic waves. The electromagnetic variety of such substance on earth lies in the infrared section. Polymer processing, space knowledge, manufacture of glass and heating a room by the open hearth fire are number of useful applications of radiation. Revankar [25] proposed the contact of free convective magnetohydrodynamic motion transversely a vertical plate by suction or injection. The thermal transport aspects of the flow caused by a stretched sheet were reported by Chiam [26]. Hayat et al. [27] reported the Darcy–Forchheimer motion of Newtonian fluid outstanding to the stretching of curved geometry with heat transport.

Chemical reaction is prominent in a number of measures in the vein of chemical indulgence, hydrometallurgical manufacturing, rubbery padding, atmospheric motions, damage of crops for the reason that of freezing, water and air pollutions, manufacture of earthenware and polymer, fog configuration and spreading etc. Ahmed [28] and Sandeep [29] investigated the scenery of chemically spontaneous motion over a vertical plate underneath different background. Ramesh Babu et al. [30, 31] reported the motion of viscous fluid with chemical reaction. Misra et al. [32] analyzed the stretching motion of viscoelastic fluid among non homogeneous heat source/sink in addition to chemical reaction.

In this object a mathematical sculpts has been projected and analysed to study the manipulate of chemical reaction and thermal radiation on MHD Williamson fluid motion above an exponentially stretching plane through heat generation and suction. Homotopic algorithm [33-37] is developed to locate the expressions of flow, temperature and concentration. Convergence of the developed sequence solutions is confirmed.

2. MATHEMATICAL FORMULATION

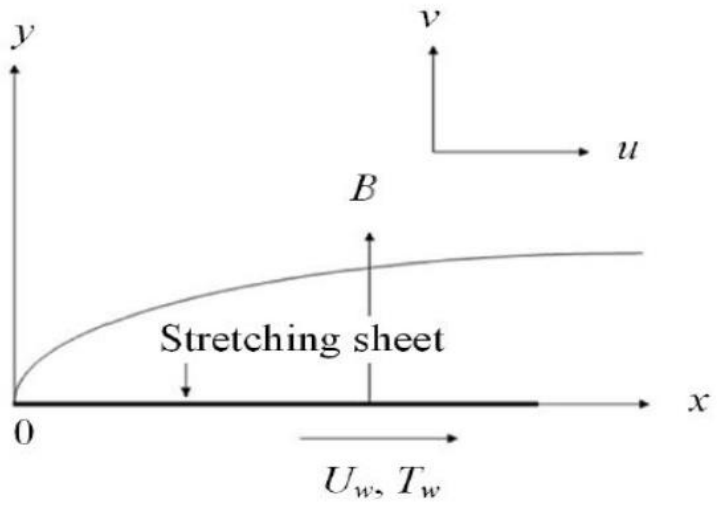

Fig. I Physical Model of the motion

This debate is executed by allowing for some presumptions, incorporating steady, two dimensional and incompressible radiative and dissipative Williamson fluid over a chemically reactive exponential porous stretching sheet under heat generation and suction with stretching velocity $U_w = U_0 e^{\frac{Nx}{L}}$. A changeable magnetic field $B = B_0 e^{\frac{Nx}{2L}}$ is functional normal to the sheet (see Fig. I). A minute magnetic Reynolds number exists in the stream section due to the appearance of minute induced magnetic field. We utilize heat source coefficient $Q^* = Q_0 e^{\frac{Nx}{L}}$ and also chemical reaction $k_1 = k_o e^{\frac{Nx}{L}}$ in the motion region. Under these assumptions the leading border stratum equations are known by

$$\frac{\partial u}{\partial x} + \frac{\partial v}{\partial y} = 0, \tag{1}$$

$$u\frac{\partial u}{\partial x} + v\frac{\partial u}{\partial y} = \nu\frac{\partial^2 u}{\partial y^2} + \sqrt{2}\nu\Gamma\frac{\partial u}{\partial y}\frac{\partial^2 u}{\partial y^2} + g\,\beta_T\left(T - T_\infty\right) + g\,\beta_C\left(C - C_\infty\right) - \frac{\sigma B^2 u}{\rho}, \tag{2}$$

$$u\frac{\partial T}{\partial x} + v\frac{\partial T}{\partial y} = \frac{k}{\rho C_p}\frac{\partial^2 T}{\partial y^2} - \frac{1}{\left(\rho C_p\right)}\frac{\partial q_r}{\partial y} - \frac{1}{\left(\rho C_p\right)}Q^*\left(T - T_\infty\right), \tag{3}$$

$$u\frac{\partial C}{\partial x} + v\frac{\partial C}{\partial y} = D_B\frac{\partial^2 C}{\partial y^2} - k_1\left(C - C_\infty\right). \tag{4}$$

Theme to the border conditions

$$\left.\begin{array}{ll} u = U_w,\ v = -V(x),\ T = T_w = \mathrm{T}_\infty + \mathrm{T}_0 \mathrm{e}^{\frac{2Nx}{L}},\ C = C_w = \mathrm{C}_\infty + \mathrm{C}_0 \mathrm{e}^{\frac{2Nx}{L}} & at\ y = 0, \\ u \to 0, \quad T \to T_\infty, \quad C \to C_\infty & as\ y \to \infty, \end{array}\right\} \tag{5}$$

where u and v are the motion components in the x and y directions correspondingly, ν is the kinematic viscosity, $\Gamma > 0$ is the time rate constant, β_T is the thermal expansion coefficient, β_C is the concentration expansion coefficient, g is the acceleration due to gravity, σ is the electrical conductivity of the fluid, ρ is the fluid density, $B(x) = B_0 e^{\frac{Nx}{2L}}$ is the variable magnetic field strength, k is the thermal conductivity, T is the fluid temperature, C is the fluid concentration, T_∞, C_∞ are the temperature and concentration of the fluid in the free stream, C_p is the specific heat at constant pressure, q_r is the radiative heat flux, $Q^* = Q_0 e^{\frac{Nx}{L}}$ is the heat generation/absorption coefficient, D_B is the Brownian diffusion coefficient and $k_1 = k_o e^{\frac{Nx}{L}}$ is the chemical reaction rate coefficient, L is the reference length, N is the exponential parameter, $V(x) = v_0 e^{\frac{Nx}{2L}}$ is the velocity of suction, v_0 is the strength of suction velocity.

Underneath Rosseland estimate, the radiative heat flux is

$$q_r = -\frac{4\sigma^*}{3k^*}\frac{\partial T^4}{\partial y},$$

where σ^* is the Stefan-Boltzman constant and k^* is the mean absorption coefficient. Further, we presume that the temperature difference within the stream is such that T^4 is uttered as a linear function of temperature. Hence, expanding T^4 in Taylor series about T_∞ and neglecting higher order terms, we obtain

$$\mathrm{T}^4 \cong 4T_\infty^3 T - 3T_\infty^4.$$

Now, we set up the similarity transformations:

$$\left.\begin{array}{l} u = U_0 e^{\frac{Nx}{L}} f'(\zeta),\ \zeta = y\sqrt{\frac{U_0}{2\nu L}} e^{\frac{Nx}{2L}},\ v = -\sqrt{\frac{U_0 \nu}{2L}} e^{\frac{Nx}{2L}} N\left(f(\zeta) + \zeta f'(\zeta)\right), \\ T = T_\infty + T_0 e^{\frac{2Nx}{L}} \theta(\zeta),\ C = C_\infty + C_0 e^{\frac{2Nx}{L}} \phi(\zeta), \end{array}\right\} \tag{6}$$

Substituting Equation (6) in Equations (2) to (5), we achieve

$$f'''+\lambda f''f'''+N\left(ff''-2f'^{2}\right)+2Gr\,\theta+2Gc\,\phi-M\,f'=0, \tag{7}$$

$$\frac{1}{\Pr}\left(1+\frac{4}{3}R\right)\theta''+N\left(f\theta'-4f'\theta\right)+Q\theta=0, \tag{8}$$

$$\phi''+N\,Le\left(f\phi'-4f'\phi\right)-Le\,\gamma\phi=0. \tag{9}$$

The border situation are

$$\begin{aligned} &f=S, \quad f'=1, \quad \theta=1, \quad \phi=1 \quad at \quad \zeta=0,\\ &f'\to 0, \quad \theta\to 0 \quad \phi\to 0 \quad as \quad \zeta\to\infty, \end{aligned} \tag{10}$$

where $\lambda=\Gamma\sqrt{\frac{U_0^3 e^{\frac{3Nx}{L}}}{\nu L}}$ is the Williamson fluid factor, $Gr=\frac{g\beta_T T_0 L}{U_0^2}$ is the thermal Grashof number, $Gc=\frac{g\beta_C C_0 L}{U_0^2}$ is the concentration Grashof number, $M=\frac{2L\sigma B_0^2}{\rho U_0}$ is the magnetic factor, $K=\frac{2\nu L}{k_p U_w}$ is the porosity factor, $Pr=\frac{\rho C_p \nu}{k}$ is the Prandtl number, $R=\frac{4\sigma^* T_\infty^3}{k^* k}$ is the radiation factor, $Q=\frac{Q_0 L}{\rho C_p U_0}$ is the heat generation/absorption factor, $Le=\frac{\nu}{D_B}$ is the Lewis number, $\gamma=\frac{k_0 L}{U_0}$ is the chemical reaction factor, $S=\frac{v_0}{\sqrt{\frac{U_0\nu}{2L}}}$ is the suction factor.

Non-dimensional friction factor C_f, local heat transport rate Nu_x and local mass transport rate Sh_x are

$C_f=\frac{2\tau_w}{\rho U_0^2 e^{2x/L}}$, where $\tau_w=\left(\mu\left(\frac{\partial u}{\partial y}\right)+\frac{\Gamma}{\sqrt{2}}\left(\frac{\partial u}{\partial y}\right)^2\right)_{y=0}$,

$Nu_x=\frac{xq_w}{k\left(T_w-T_\infty\right)}$ and $Sh_x=\frac{xq_m}{D_B\left(C_w-C_\infty\right)}$,

where q_w and q_m are the heat and mass fluxes at the surface correspondingly specified by

$q_w = \left(-\left(k + \frac{16\sigma^* T_\infty^3}{3k^*} \right) \left(\frac{\partial T}{\partial y} \right) \right)_{y=0}$, $q_m = -D_B \left(\frac{\partial C}{\partial y} \right)_{y=0}$.

Substituting q_w and q_m in the former equations, we obtain

$\mathrm{Re}_x^{1/2} C_f = \left(f''(0) + \frac{\lambda}{2} \left(f''(0) \right)^2 \right)$, $(Re_x)^{-1/2} Nu_x = -\left(1 + \frac{4}{3} R \right) \theta'(0)$ and

$(Re_x)^{-1/2} Sh_x = -\phi'(0)$, where $Re_x = \frac{U_w x}{\nu}$ is the local Reynolds number.

3. HAM

Here, we state the modus operandi to collect the solutions of the Equations (7) to (10) by means of HAM. We handle onto the initial guesses f_0, θ_0 and ϕ_0 of f, θ and ϕ as

$f_0(\zeta) = S + 1 - e^{-\zeta}$,
$\theta_0(\zeta) = e^{-\zeta}$,
$\phi_0(\zeta) = e^{-\zeta}$.

The linear operators are particular as

$L_1(f) = f''' - f'$,
$L_2(\theta) = \theta'' - \theta$,
$L_3(\phi) = \phi'' - \phi$,

with the following properties

$L_1\left(C_1 + C_2 e^{\zeta} + C_3 e^{-\zeta} \right) = 0$,
$L_2\left(C_4 e^{\zeta} + C_5 e^{-\zeta} \right) = 0$,
$L_3\left(C_6 e^{\zeta} + C_7 e^{-\zeta} \right) = 0$,

where C_i $(i = 1 \text{ to } 7)$ are the arbitrary constants.

If $p \in [0,1]$ is the embedding factor, h_1, h_2 and h_3 are the non-zero auxiliary factor, then we set up the following zeroth-order deformation equations as

$$(1-p) L_1\left(f(\zeta; p) - f_0(\zeta) \right) = p h_1 N_1\left[f(\zeta; p), \theta(\zeta; p), \phi(\zeta; p) \right], \tag{11}$$

$$(1-p)L_2\left(\theta(\zeta;p)-\theta_0(\zeta)\right)=p\,h_2\,N_2\left[f(\zeta;p),\theta(\zeta;p),\phi(\zeta;p)\right], \tag{12}$$

$$(1-p)L_3\left(\phi(\zeta;p)-\phi_0(\zeta)\right)=p\,h_3\,N_3\left[f(\zeta;p),\theta(\zeta;p),\phi(\zeta;p)\right] \tag{13}$$

subject to the border circumstances

$$\begin{aligned} &f(0;p)=S, && f'(0;p)=1, && f'(\infty;p)=0,\\ &\theta(0;p)=1, && && \theta(\infty;p)=0,\\ &\phi(0;p)=1, && && \phi(\infty;p)=0. \end{aligned} \tag{14}$$

We define the nonlinear operators as

$$\begin{aligned} N_1\left[f(\zeta;p),\theta(\zeta;p),\phi(\zeta;p)\right]&=\frac{\partial^3 f(\zeta;p)}{\partial\zeta^3}+\lambda\frac{\partial^2 f(\zeta;p)}{\partial\zeta^2}\frac{\partial^3 f(\zeta;p)}{\partial\zeta^3}\\ &+N\left(f(\zeta;p)\frac{\partial^2 f(\zeta;p)}{\partial\zeta^2}-2\left(\frac{\partial f(\zeta;p)}{\partial\zeta}\right)^2\right)+2Gr\,\theta(\zeta;p)+2Gr\,\varphi(\zeta;p)-M\frac{\partial f(\zeta;p)}{\partial\zeta}, \end{aligned} \tag{15}$$

$$\begin{aligned} N_2\left[f(\zeta;p),\theta(\zeta;p),\phi(\zeta;p)\right]&=\frac{1}{\Pr}\left(1+\frac{4}{3}R\right)\frac{\partial^2\theta(\zeta;p)}{\partial\zeta^2}\\ &+N\left(f(\zeta;p)\frac{\partial\theta(\zeta;p)}{\partial\zeta}-4\frac{\partial f(\zeta;p)}{\partial\zeta}\theta(\zeta;p)\right)+Q\theta(\zeta;p), \end{aligned} \tag{16}$$

$$\begin{aligned} N_3\left[f(\zeta;p),\theta(\zeta;p),\phi(\zeta;p)\right]&=\frac{\partial^2\phi(\zeta;p)}{\partial\zeta^2}\\ &+N\,Sc\left(f(\zeta;p)\frac{\partial\phi(\zeta;p)}{\partial\zeta}-4\frac{\partial f(\zeta;p)}{\partial\zeta}\phi(\zeta;p)\right)-Sc\,\gamma\,\phi(\zeta;p), \end{aligned} \tag{17}$$

When $p=0$ and $p=1$, we obtain

$$\begin{aligned} &f(\zeta;0)=f_0(\zeta) && f(\zeta;1)=f(\zeta),\\ &\theta(\zeta;0)=\theta_0(\zeta) && \theta(\zeta;1)=\theta(\zeta),\\ &\phi(\zeta;0)=\phi_0(\zeta) && \phi(\zeta;1)=\phi(\zeta). \end{aligned} \tag{18}$$

Thus, as p advances from 0 to 1 then $f(\zeta;p)$, $g\theta(\zeta;p)$ and $\phi(\zeta;p)$ amend from initial approximations to the exact solutions of the original nonlinear differential equations.

Now, explicating $f(\zeta;p)$, $\theta(\zeta;p)$ and $\phi(\zeta;p)$ in Taylor's series w.r.to p, we have

$$f(\zeta;p)=f_0(\zeta)+\sum_{m=1}^{\infty}f_m(\zeta)\,p^m, \tag{19}$$

$$\theta(\zeta;p)=\theta_0(\zeta)+\sum_{m=1}^{\infty}\theta_m(\zeta)\,p^m, \tag{20}$$

$$\phi(\zeta;p)=\phi_0(\zeta)+\sum_{m=1}^{\infty}\phi_m(\zeta)\,p^m, \tag{21}$$

where

$$\begin{aligned} f_m(\zeta)&=\frac{1}{m!}\frac{\partial^m f(\zeta;p)}{\partial p^m}\bigg|_{p=0},\\ \theta_m(\zeta)&=\frac{1}{m!}\frac{\partial^m \theta(\zeta;p)}{\partial p^m}\bigg|_{p=0}, \\ \phi_m(\zeta)&=\frac{1}{m!}\frac{\partial^m \phi(\zeta;p)}{\partial p^m}\bigg|_{p=0}. \end{aligned} \tag{22}$$

If the parameters are opted in such a way that the series (19) to (21) are convergent at $p=1$, then

$$f(\zeta)=f_0(\zeta)+\sum_{m=1}^{\infty}f_m(\zeta), \tag{23}$$

$$\theta(\zeta)=\theta_0(\zeta)+\sum_{m=1}^{\infty}\theta_m(\zeta), \tag{24}$$

$$\phi(\zeta)=\phi_0(\zeta)+\sum_{m=1}^{\infty}\phi_m(\zeta). \tag{25}$$

Differentiating Equations (11) to (13) m times w.r.to p, setting $p=0$ and finally dividing with $m!$, we get the mth-order deformation equations as follows

$$L_1\left(f_m(\zeta)-\chi_m\, f_{m-1}(\zeta)\right)=h_1\,R_m^f(\zeta), \tag{26}$$

$$L_2\left(\theta_m(\zeta)-\chi_m\,\theta_{m-1}(\zeta)\right)=h_2\,R_m^\theta(\zeta), \tag{27}$$

$$L_3\left(\phi_m(\zeta)-\chi_m\,\phi_{m-1}(\zeta)\right)=h_3\,R_m^\phi(\zeta), \tag{28}$$

with the following border conditions

$$\begin{aligned} &f_m(0)=0, \qquad f_m'(0)=0, \quad f_m'(\infty)=0,\\ &\theta_m(0)=0, \qquad\qquad \theta_m(\infty)=0,\\ &\phi_m(0)=0, \qquad\qquad \phi_m(\infty)=0, \end{aligned} \tag{29}$$

where

$$R_m^f(\zeta)=f_{m-1}'''+\lambda\sum_{i=0}^{m-1}f_{m-1-i}''f_i'''+N\left(\sum_{i=0}^{m-1}f_{m-1-i}f_i''-2\sum_{i=0}^{m-1}f_{m-1-i}'f_i'\right)+2Gr\,\theta_{m-1}+2Gc\,\phi_{m-1}-M\,f_{m-1}',$$

$$R_m^\theta(\zeta)=\frac{1}{\Pr}\left(1+\frac{4R}{3}\right)\theta_{m-1}''+N\sum_{i=0}^{m-1}\left(f_{m-1-i}\theta_i'-4f_{m-i-1}'\theta_i\right)+Q\,\theta_{m-1}, \tag{31}$$

$$R_m^\phi(\zeta)=\phi_{m-1}''+N\,Sc\left(\sum_{i=0}^{m-1}f_{m-1-i}\phi_i'-4f_{m-1-i}'\phi_i\right)-Sc\,\gamma\,\phi_{m-1}, \tag{32}$$

$$\chi_m=\begin{cases}0, & m\le 1,\\ 1, & m>1.\end{cases} \tag{33}$$

4. CONVERGENCE OF HAM SOLUTION

To heap up the well-matched values for these factors, h-curves are delineated in Fig. 1. From this draft, it is penetrated that the persuasive section of the factors is about $[-1.2, 0.0]$. For $h_1=h_2=h_3=-0.94$, the series solutions are convergent in the whole district of ζ. Table 1 exhibit the convergence of the process.

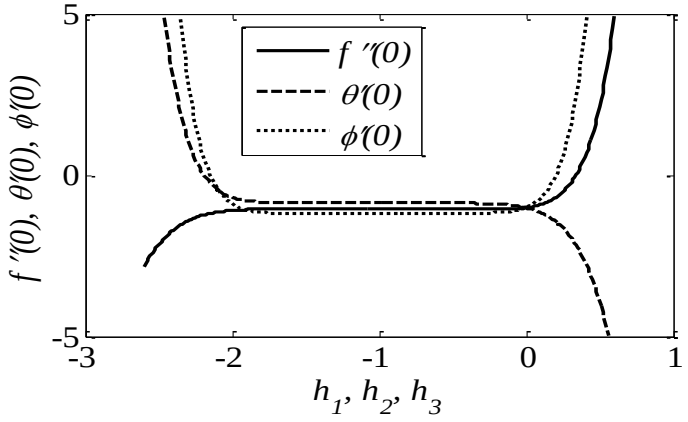

Fig. 1: $\hbar$-curves of $f''(0), \theta'(0)$ and $\phi'(0)$ for 15th order approximation.

Order	$-f''(0)$	$-\theta'(0)$	$-\phi'(0)$
5	1.050563	1.258176	1.221316
10	1.050212	1.259812	1.224151
15	1.050205	1.259761	1.224135
20	1.050196	1.259756	1.224130
25	1.050197	1.259756	1.224129
30	1.050197	1.259756	1.224129
35	1.050197	1.259756	1.224129
40	1.050197	1.259756	1.224129
45	1.050197	1.259756	1.224129

5. RESULTS AND DISCUSSION

Enormous numerical computations have been racked up for motion, thermal and concentrated profiles along with friction factor feature, Nusselt as well as Sherwood number for varietal principles of substantial values which reveals the chart of motion, heat and mass transport rate of the liquid.

In this investigation the subsequent evasion bound values are undertaken for computations: $\lambda = 0.5, N = 3.0, M = 0.7, S = 0.5, \Pr = 0.7, Gr = 0.5, Gc = 0.5, R = 0.3, Q = 0.1, Sc = 0.78, \gamma = 0.5.$

We noticed from the Fig. 1, the motion of the liquid declines with a scramble in standards of the Williamson fluid factor λ. This is owing to the fact that Williamson factor is proportion of relaxation time to the retardation time. Thus, with an augmentation in the values of Williamson stricture, imposes the relaxation time Γ, which becomes soaring since the liquid particles take more time to return their position. So, as a consequence, viscosity is improved and the velocity of the fluid particles declines. Also, thermal and concentration outlines amplify with Williamson constraint. This is exposed in Figs. 3 and 4. The impact of magnetic constraint M on motion of the liquid is exposed by Fig. 5 which demonstrates that a boost in M diminishes the motion of the profile. This is due to Lorentz force that acts as a retarding force. Such force increases the frictional resistance opposing the liquid motion in momentum border stratum width, while reverse marks were observed in case of thermal and concentration which were exposed in Figs. 6 and 7.

The influence of exponential constraint N on motion, thermal and concentration distributions is exhibited in Figs. 8 to 10 correspondingly. It is apparent that an increase in the constraints of exponential diminishes motion of liquid, thermal and concentration characteristics. Figs. 11-12 exploit the manipulate of thermal Grashof quantity on motion of the liquid and thermal outlines. An amplifying in Gr constraints which pilots to amplify in momentum of the motion profile and diminishes in thermal outline respectively. Raises in the constraints of mass Grashof values leads to the enhance in motion border stratum thickness and diminish in concentration border stratum width. This is exposed in Figs. 13-14. The important of suction S is to fetch the fluid closer to the surface and hence lessen the momentum border stratum width. This is revealed in Fig. 15. As it can be apparent from the Fig. 16, that the thermal border of motion field is a downhill function of $\Pr$. The control of radiation constraint R on thermal is shown in Fig. 17. It can be pragmatic that there is an augmentation in the temperature with an increase in radiation constraint. This may occurs due to the fact that amplifies in the radiation parameter produces heat energy in the motion region. Due to the dominion of exterior heat compared with the heat source supplied to the motion, we observed enhancement of temperature with the raise of heat source Q. This is portrayed in Fig. 18. Fig. 19 elucidates that $\phi(\zeta)$ decreases as Schmidt quantity Sc increases. The substantial quarrel behind this is the boost in Sc implies reduce in molecular diffusivity which as a result reduces concentration outline and mass transport rate. Behavior of chemically reactive constraint Kr on $\phi(\zeta)$ is observed in Fig. 20. We visualized that $\phi(\zeta)$ and thickness of associated stratum are diminishing as boost of Kr.

Figs. 21-23 exhibit the influence of friction factor, local rate of heat transport (Nusselt number) and local rate of mass transport (Sherwood number).

Fig. 21 demonstrates results of wall shear stress with magnetic constraints and exponential constraints. Local skin friction decreases with the increase in *M* and *N*. Local Nusselt number increases with the increase *N* and reduces with thermal radiation constraints *R* (see Fig. 22). Local Sherwood number increases with the increase in both chemical reaction factor and exponential factor (see Fig. 23).

Table 1 is constructed for comparative study of present results with those of previous results for various values of M and shows good agreement with each other.

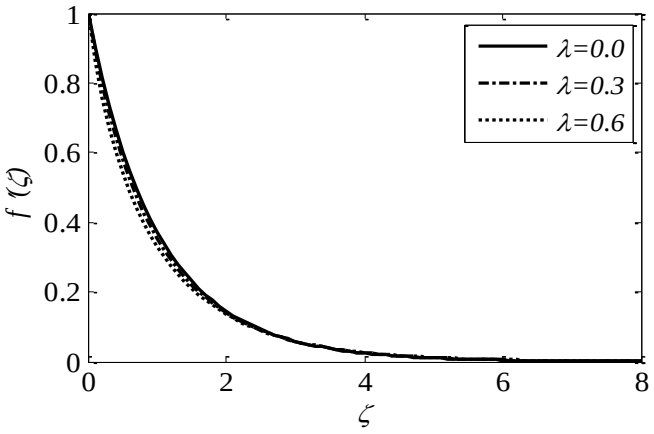

Fig. 2. Effect of λ on $f'(\zeta)$.

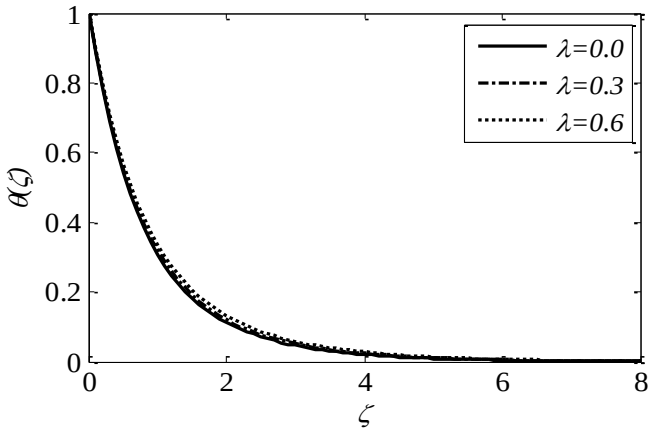

Fig. 3. Effect of λ on $\theta(\zeta)$.

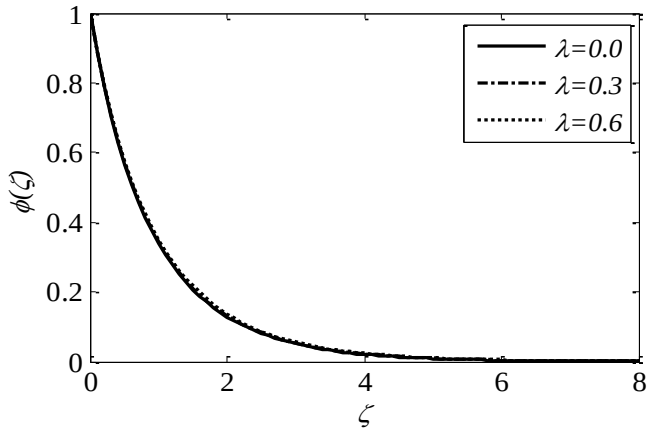

Fig. 4. Effect of λ on $\phi(\zeta)$.

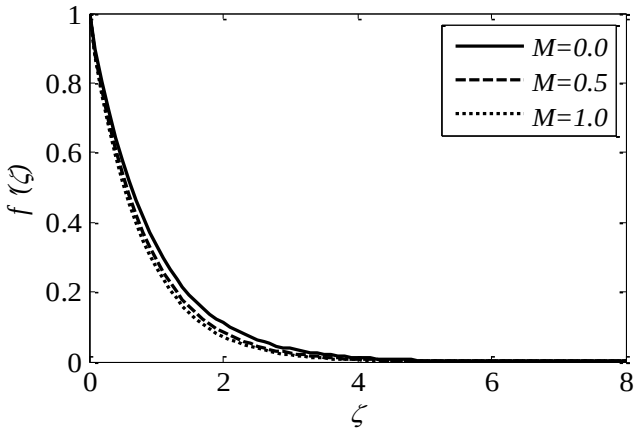

Fig. 5. Effect of M on $f'(\zeta)$.

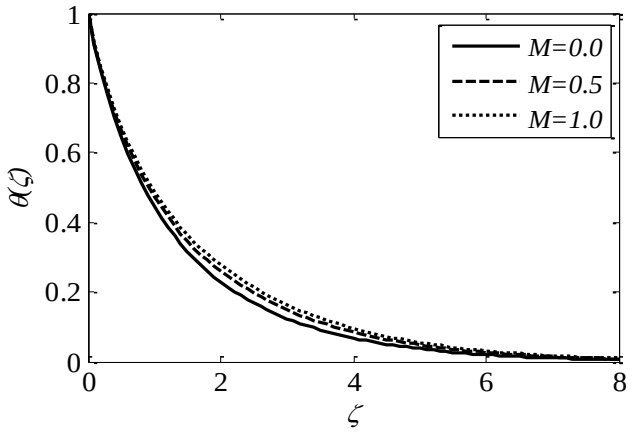

Fig. 6. Effect of M on $\theta(\zeta)$.

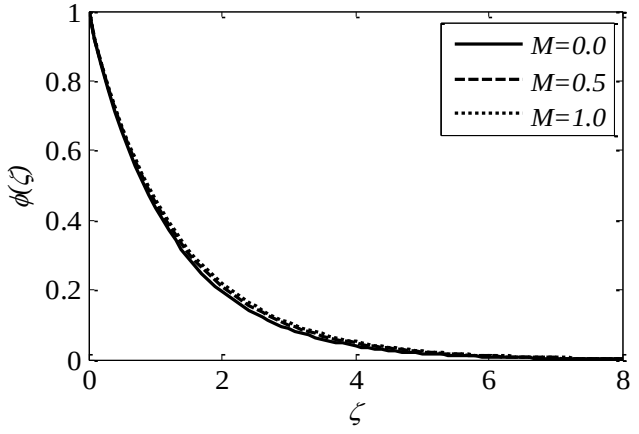

Fig. 7. Effect of M on $\phi(\zeta)$.

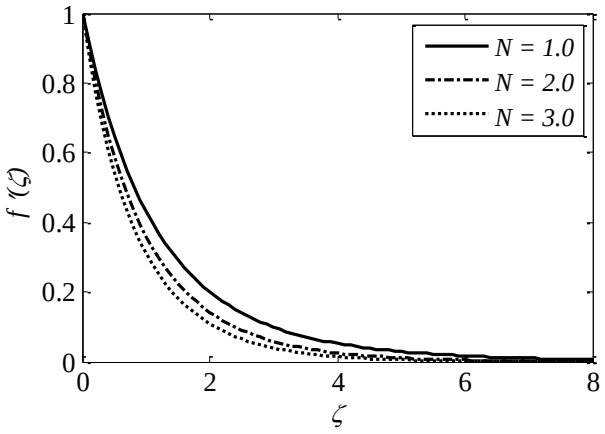

Fig. 8. Effect of N on $f'(\zeta)$.

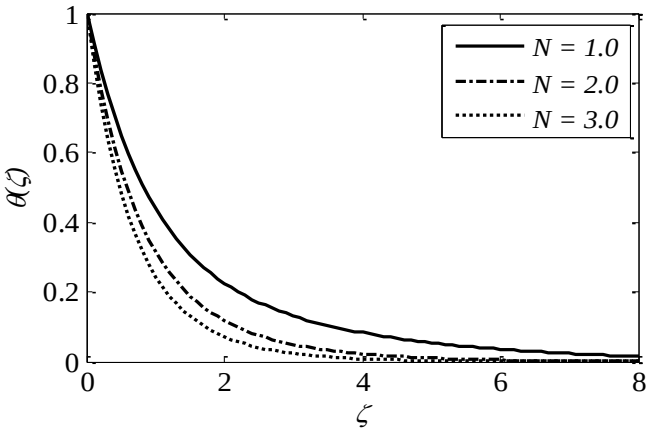

Fig. 9. Effect of N on $\theta(\zeta)$.

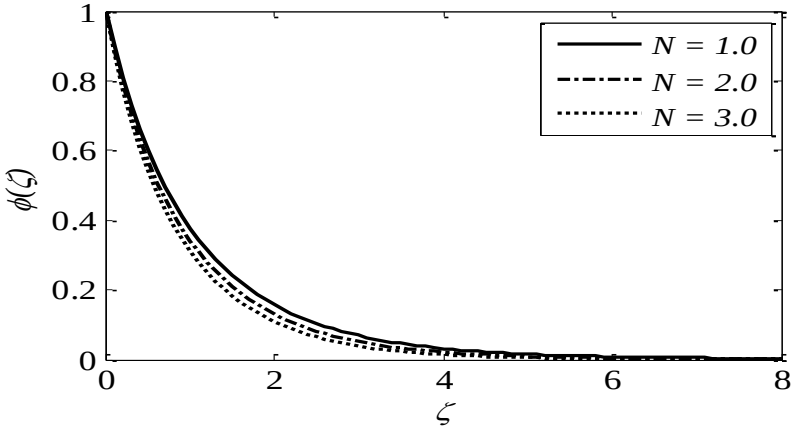

Fig. 10. Effect of N on $\phi(\zeta)$.

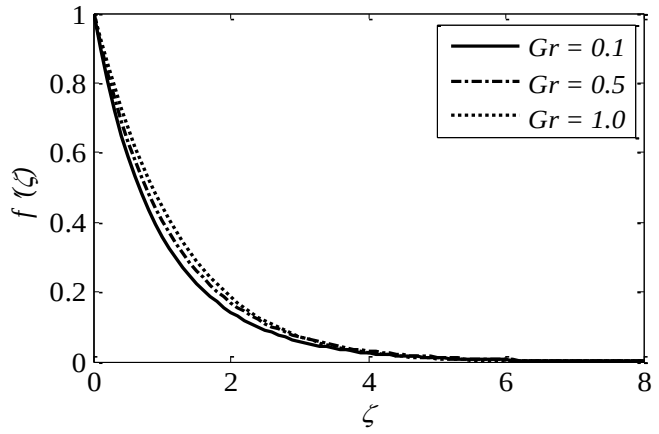

Fig. 11. Effect of Gr on $f'(\zeta)$.

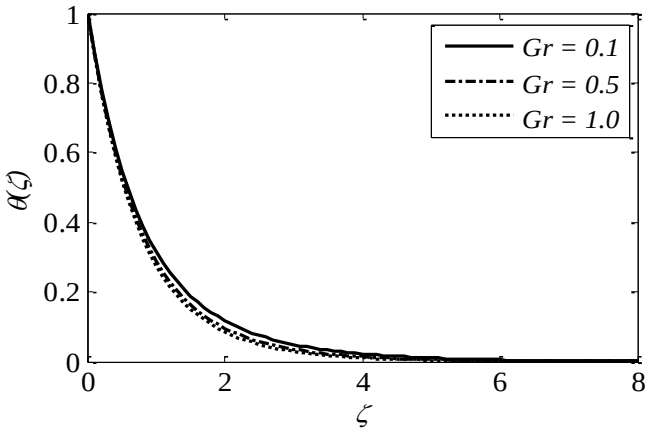

Fig. 12. Effect of Gr on $\theta(\zeta)$.

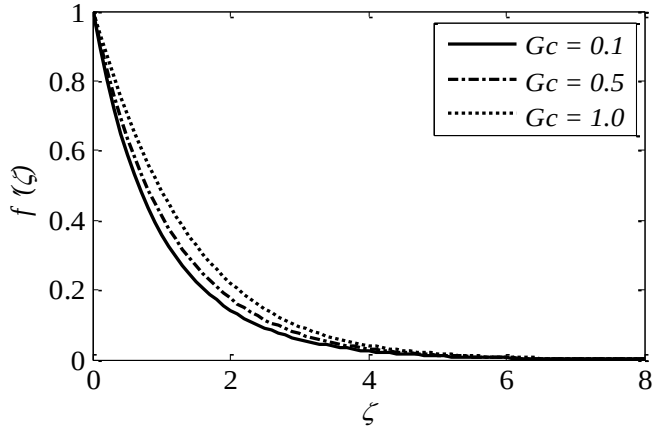

Fig. 13. Effect of Gc on $f'(\zeta)$.

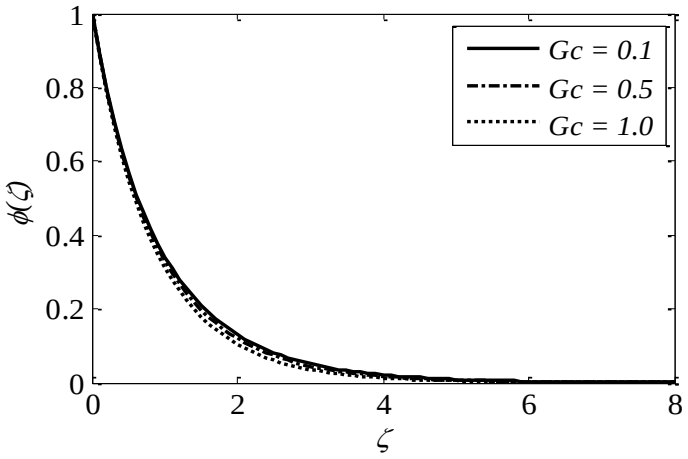

Fig. 14. Effect of Gc on $\phi(\zeta)$

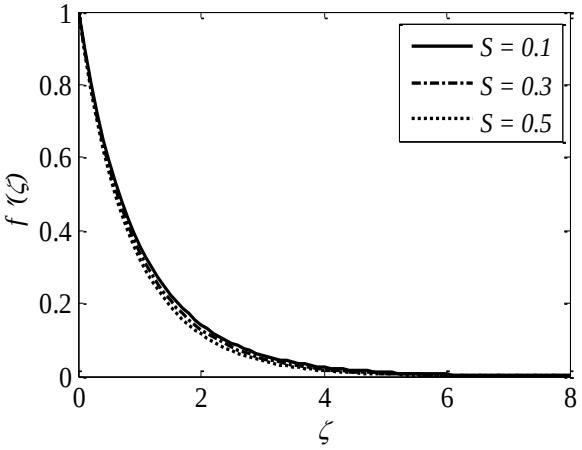

Fig. 15. Effect of S on $f'(\zeta)$.

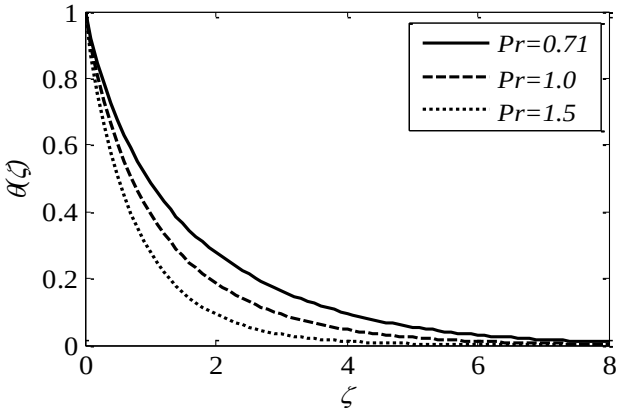

Fig. 16. Effect of Pr on $\theta(\zeta)$.

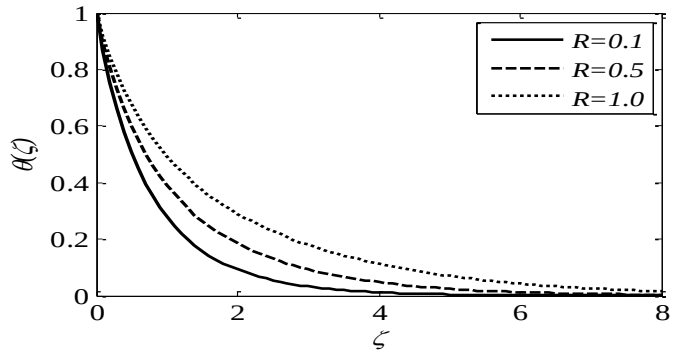

Fig. 17. Effect of R on $\theta(\zeta)$.

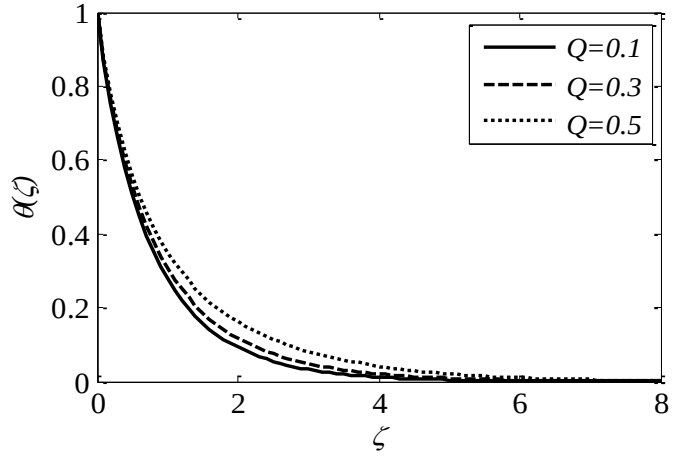

Fig. 18. Effect of Q on $\theta(\zeta)$.

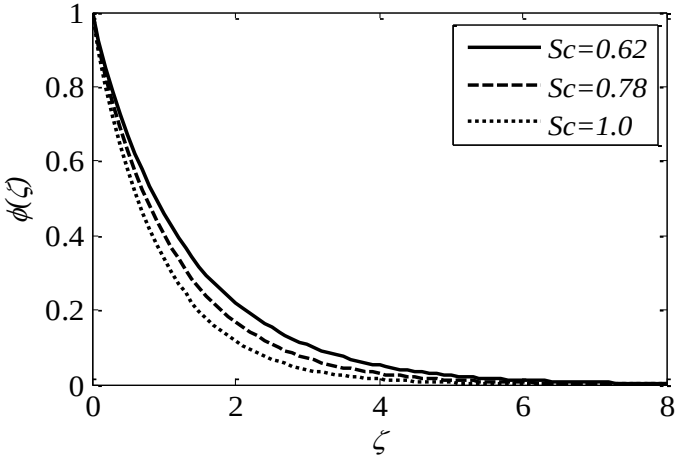

Fig. 19. Effect of Sc on $\phi(\zeta)$.

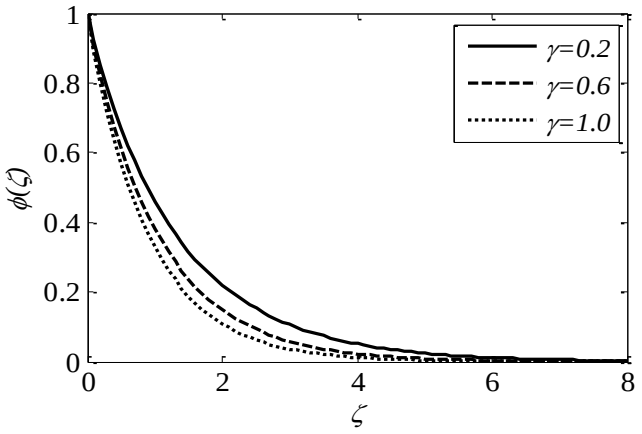

Fig. 20. Effect of γ on $\phi(\zeta)$.

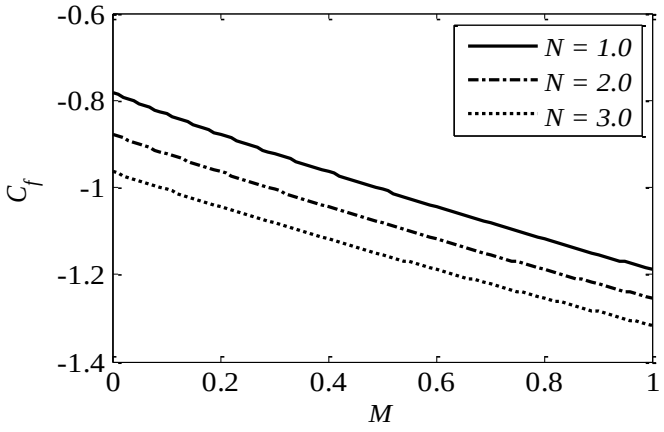

Fig. 21 Effect of M and N on C_f.

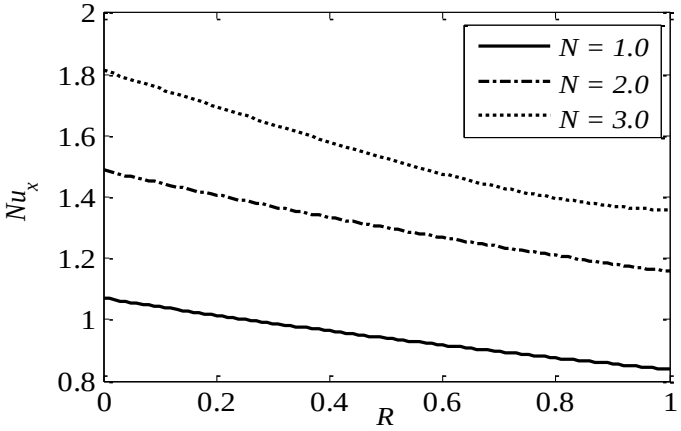

Fig. 22 Effect of R and N on Nu_x.

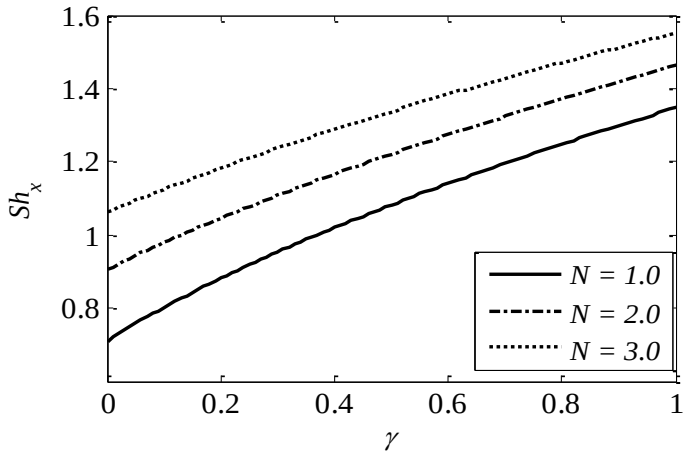

Fig. 23 Effect of γ and N on Sh_x.

Table 1. Comparison of $-f''(0)$ when $Gr = Gc = S = 0.0, N = 1.0.$

M	Kameswaran et al. [38]	HAM
0.0	1.281809	1.281801
1.0	1.629178	1.629172

4. CONCLUSIONS

This paper deals with the heat and mass transport effects on Williamson fluid motion across an exponential stretching sheet with radiation, suction and chemical reaction. The impact of different non-dimensional parameters on the three usual profiles (velocity, temperature and concentration) together with friction factor, local Nusselt and Sherwood numbers are reported through plots and table. The foremost conclusions are as follows:

- Increasing values of exponential parameter reduces velocity fields.
- The fluid velocity maintains an inverse relationship with Williamson fluid factor but an inverse result is found in thermal and concentration fields.
- A rise in thermal Grashof (mass Grashof) number increases motion of the fluid, and decreases thermal (concentration) border stratums.
- The same effect is observed on the temperature profile and concentration profile with enlarged values of the exponential parameter.
- The same effect is noticed on Nusselt and Sherwood numbers with exponential parameter.

CONFLICT OF INTERESTS

The authors declare that there is no conflict of interests.

REFERENCES

[1] R.V. Williamson, The flow of pseudoplastic materials, Ind. Eng. Chem. 21 (1929), 1108-1111.

[2] S. Nadeem and S.T. Hussian, Heat transfer analysis of Williamson fluid over exponentially stretching surface, Appl. Math. Mech. 35 (2014), 489-502.

[3] D. Pal, N. Roy, K. Vajravelu, Effects of thermal radiation and Ohmic dissipation on MHD Casson nanofluid flow over a vertical non-linear stretching surface using scaling group transformation, Int. J. Mech. Sci. 114 (2016) 257–267.

[4] S. Reddy C, K. Naikoti, M.M. Rashidi, MHD flow and heat transfer characteristics of Williamson nanofluid over a stretching sheet with variable thickness and variable thermal conductivity, Trans. A. Razmadze Math. Inst. 171 (2017), 195–211.

[5] M.Y. Malik, T. Salahuddin, Numerical solution of MHD stagnation point flow of Williamson fluid model over a stretching cylinder, Int. J. Nonlinear Sci. Numer. Simul. 16 (2015), 161-164.

[6] R.P. Sharma, K. Avinash, N. Sandeep, O.D. Makinde, Thermal Radiation Effect on Non-Newtonian Fluid Flow over a Stretched Sheet of Non-Uniform Thickness, Defect Diffusion Forum. 377 (2017), 242–259.

[7] G. Kumaran, N. Sandeep, R. Vijayaragavan, Melting heat transfer in magnetohydrodynamic radiative Williamson fluid flow with non-uniform heat source/sink, IOP Conf. Ser., Mater. Sci. Eng. 263 (2017), 062022.

[8] R.C. Lessmann, W. M. Hagist, Turbulent separated and reattached flow over a curved surface, J. Fluids Eng. 109 (1987), 403-409.

[9] R.W. Barber, Y. Sun, X.J. Gu, D.R. Emerson, Isothermal slip flow over curved surfaces, Vacuum. 76 (2004), 73–81.

[10] H. Xu, S.J. Liao, Laminar flow and heat transfer in the boundary-layer of non-Newtonian fluids over a stretching flat sheet, Comput. Math. Appl. 57 (2009), 1425–1431.

[11] M. Sajid, N. Ali, T. Javed, Z. Abbas, Stretching a Curved Surface in a Viscous Fluid, Chin. Phys. Lett. 27 (2010), 024703.

[12] M. Naveed, Z. Abbas, M. Sajid, et al. Dual Solutions in Hydromagnetic Viscous Fluid Flow Past a Shrinking Curved Surface. Arab J. Sci. Eng. 43 (2018), 1189–1194.

[13] T. Hayat, R. Sajjad, R. Ellahi, T. Muhammad, B. Ahmad. Numerical study for Darcy-Forchheimer flow due to a curved stretching surface with Cattaneo-Christov heat flux and homogeneous-heterogeneous reactions. Res. Phys. 7 (2017), 2886-2892.

[14] S.H.M. Saleh, N.M. Arifin, R. Nazar, I. Pop, Unsteady Micropolar Fluid over a Permeable Curved Stretching Shrinking Surface, Math. Probl. Eng. 2017 (2017), 3085249.

[15] N.F. Okechi, M. Jalil, S. Asghar. Flow of viscous fluid along an exponentially stretching curved surface. Res. Phys. 7 (2017), 2851–2854.

[16] M. Subhas Abel, E. Sanjayanand, M.M. Nandeppanavar, Viscoelastic MHD flow and heat transfer over a stretching sheet with viscous and ohmic dissipations, Commun. Nonlinear Sci. Numer. Simul. 13 (2008) 1808–1821.

[17] V. Kumaran, A.K. Banerjee, A. Vanav Kumar, K. Vajravelu, MHD flow past a stretching permeable sheet, Appl. Math. Comput. 210 (2009), 26–32.

[18] F. Mabood, W.A. Khan, A.I.Md. Ismail, MHD flow over exponential radiating stretching sheet using homotopy analysis method, J. King Saud Univ., Eng. Sci. 29 (2017), 68–74.

[19] S. Sheri, A. Chamkha, A. Suram, Heat and Mass Transfer Effects on MHD Natural Convection Flow Past an Impulsively Moving Vertical Plate with Ramped Temperature, Amer. J. Heat Mass Transfer. 3 (2016), 129-148.

[20] K.V. Prasad, K. Vajravelu, H. Vaidya, Hall effect on MHD flow and heat transfer over a stretching sheet with variable thickness, Int. J. Comput. Meth. Eng. Sci. Mech. 17 (2016), 288–297.

[21] R. Cortell, Fluid flow and radiative nonlinear heat transfer over a stretching sheet. J. King Saud Univ. Sci. 26 (2014), 161–167.

[22] M. Sheikholeslami, S. Abelman, D.D. Ganji, Numerical simulation of MHD nanofluid flow and heat transfer considering viscous dissipation, Int. J. Heat Mass Transfer. 79 (2014), 212–222.

[23] M.G. Reddy, P. Padma, B. Shankar, Effects of viscous dissipation and heat source on unsteady MHD flow over a stretching sheet, Ain Shams Eng. J. 6 (2015), 1195–1201.

[24] S.M. Ibrahim, P.V. Kumar, CSK. Raju, Possessions of viscous dissipation on radiative MHD heat and mass transfer flow of a micropolar fluid over a porous stretching sheet with chemical reaction, Trans. Phenom. Nano Micro Scales, 6(2018), 60-71.

[25] S.T. Revankar, Natural convection effects on MHD flow past an impulsively started permeable vertical plate, Indian J. Pure Appl. Math. 14 (1983), 530–539.

[26] T.C. Chiam, Heat transfer in a fluid with variable thermal conductivity over a linearly stretching sheet. Acta Mech. 129 (1998), 63–72.

[27] T. Hayat, F. Haider, T. Muhammad, A. Alsaedi, Darcy-Forchheimer flow due to a curved stretching surface with Cattaneo-Christov double diffusion: A numerical study, Res. Phys. 7 (2017), 2663–2670.

[28] A. Sahin, Influence of chemical reaction on transient mhd free Convective flow over a vertical plate in slip-flow Regime. Emirates J. Eng. Res. 15 (1) (2010), 25-34.

[29] N. Sandeep, A.V.B. Reddy, V. Sugunamma, Effect of radiation and chemical reaction on transient MHD free convective flow over a vertical plate through porous media. Chem. Proc. Eng. Res. 2 (2012), 1-9.

[30] K.R. Babu, B. Venkateswarlu, P.S. Narayana, Effects of chemical reaction and radiation on MHD flow of a viscous fluid in a vertical channel with non-uniform concentration. Int. J. Math. Comput. Sci. 2 (1) (2016), 34-42.

[31] K.R. Babu, B. Venkateswarlu, P.V. Satyanarayana, Effects of chemical reaction and radiation absorption on mixed convective flow in a circular annulus at constant heat and mass flux. Adv. Appl. Sci. Res. 5 (5) (2014), 122-138.

[32] S.R. Mishra, P.K. Pattnaik, M.M. Bhatti, T. Abbas, Analysis of heat and mass transfer with MHD and chemical reaction effects on viscoelastic fluid over a stretching sheet. Indian J. Phys. 91 (10) (2017), 1219-1227.

[33] S.M. Ibrahim, G. Lorenzini, P.V. Kumar, C.S.K. Raju, Influence of chemical reaction and heat source on dissipative MHD mixed convection flow of a Casson nanofluid over a nonlinear permeable stretching sheet. Int. J. Heat Mass Transfer. 111 (2017), 346-355.

[34] P.V. Kumar, S.M. Ibrahim, K. Jyothsna, Numerical modeling on radiative dissipative MHD flow of a chemically casson fluid over an exponentially inclined stretching surface. Math. Model. Eng. Probl. 6 (4) (2019), 491-501.

[35] S.M. Ibrahim, P.V. Kumar, G. Lorenzini, Analytical Modeling of Heat and Mass Transfer of Radiative MHD Casson Fluid over an Exponentially Permeable Stretching Sheet with Chemical Reaction. J. Eng. Thermophys. 29 (1) (2020), 136-155.

[36] S.M. Ibrahim, P.V. Kumar, O.D. Makinde, Chemical Reaction and Radiation Effects on Non-Newtonian Fluid Flow over a Stretching Sheet with Non-Uniform Thickness and Heat Source, Defect Diff. Forum, 387 (2018), 319-331.

[37] P.V. Kumar, S.M. Ibrahim, G. Lorenzini, Impact of thermal radiation and Joule heating on MHD mixed convection flow of a Jeffrey fluid over a stretching sheet using homotopy analysis method. Int. J. Heat Technol. 35 (4) (2017), 978-986.

[38] P.K. Kameswaran, M. Narayana, P. Sibanda, G. Makanda, On radiation effects on hydromagnetic Newtonian liquid flow due to an exponential stretching sheet. Bound. Value Probl. 2012 (2012), 105.

[39] G. Sreedevi, D.R.V.P. Rao, O.D. Makinde, G.V.R. Reddy, Soret and Dufour effects on MHD flow with heat and mass transfer past a permeable stretching sheet in presence of thermal radiation, Indian J. Pure Appl. Phys. 55 (8) (2017), 551-563.

[40] K.J. Reddy, N.P.M. Reddy, R.K. Konijeti, A. Dasore, Numerical Investigation of Chemical Reaction and Heat Source on Radiating MHD Stagnation Point Flow of Carreau Nanofluid with Suction/Injection. Defect Diff. Forum. 388 (2018), 171-189.

[41] P. Nagasantoshi, G. V. Ramana Reddy, M. Gnaneswara Reddy, P. Padma, Heat and Mass Transfer of Non-Newtonian Nanofluid Flow Over a Stretching Sheet with Non-Uniform Heat Source and Variable Viscosity, J. Nanofluids ,7 (5) (2018), 821-832.

[42] K. Suneetha, S.M. Ibrahim, G.V.R. Reddy, Radiation and heat source effects on MHD flow over a permeable stretching sheet through porous stratum with chemical reaction, Multidiscipline Model. Mat. Struct. 14 (5) (2018), 1101-1114.

[43] G.V.R. Reddy, Y.H. Krishna, Soret and Dufour Effects on MHD Micropolar Fluid Flow Over a Linearly Stretching Sheet, Through a Non-Darcy Porous Medium, Int. J. Appl. Mech. Eng. 23 (2) (2018), PP. 485-502

[44] M Dhanalakshmi, .V Jyothi, .K Jayarami Reddy, Soret and Dufour Effects on MHD Convective Flow Past a Vertical Plate Through Porous Medium, J. Phys.: Conf. Ser. 1344 (2019), 012008.

[45] K.J. Reddy, M.N. Reddy, K. Ramakrishna, The study of double stratification and viscous dissipation effects on chemically radiative MHD free convective flow of micropolar fluid embedded in non-Darcian porous medium, J. Phys.: Conf. Ser. 1344 (2019), 012022.

[46] K. Vijaya, G.V.R. Reddy, Magnetohydrodynamic Casson Fluid Flow Over a Vertical Porous Plate in the Presence of Radiation, Soret and Chemical Reaction Effects, J. Nanofluids. 8 (2019), 1240–1248.

[47] A. Sandhya, G.V.R. Reddy, G.V.S.R. Deekshitulu, Steady on MHD Heat and Mass Transfer Flow of an Inclined Porous Plate in the Presence of Radiation and Chemical Reaction, J. Phys.: Conf. Ser. 1344 (2019), 012002.

[48] G. Sivaiah, K.J. Reddy, P.C. Reddy, M.C. Raju, Numerical study of mhd boundary layer flow of a viscoelastic and dissipative fluid past a porous plate in the presence of thermal radiation, Int. J. Fluid Mech. Res. 46 (2019), 27–38.

[49] P. Naga Santoshi, G. Venkata Ramana Reddy, P. Padma, Numerical Study of Carreau Nanofluid Flow Under Slips, Int. J. Appl. Comput. Math. 5 (2019), 122.

[50] G.C. Kumar, K.J. Reddy, R.K. Konijeti, M.N. Reddy. Non-Uniform Heat Source/Sink and Joule Heating Effects on Chemically Radiative MHD Mixed Convective Flow of Micropolar Fluid over a Stretching Sheet in Porous Medium, Defect Diff. forum, 388 (2018), 281-302.